The Wiskott-Aldrich syndrome protein permits assembly of a focused immunological synapse enabling sustained T-cell receptor signaling

Ronan Calvez,[1,2] Fanny Lafouresse,[1,2] Julie De Meester,[1,2] Anne Galy,[3] Salvatore Valitutti,[1,2] and Loïc Dupré [1,2]

[1]INSERM, U1043, Toulouse, France; [2]Université Toulouse III Paul-Sabatier, Centre de Physiopathologie de Toulouse Purpan, Toulouse, France and [3]INSERM, U951, Généthon, Evry, France

Acknowledgments: we are extremely grateful to the patients and their families. We thank Maria-Grazia Roncarolo and Anna Villa (San Raffaele Telethon Institute for Gene Therapy) for providing patients' samples. We wish to thank Sophie Allard and Daniel Sapede from the IFR150 microscopy platform (Toulouse). We also thank Josipa Spoljaric for manuscript editing.

Funding: this work was supported by the European Community (Marie Curie Excellence grant, contract MEXT-CT-2005-025032 to LD), by the French National Research Agency (ANR-maladies rares grant "PhysioWAS" to AG and LD) and by the Association pour la Recherche sur le Cancer ("Subvention Libre" to SV).

Manuscript received on January 7, 2011. Revised version arrived on may 16, 2011. Manuscript accepted on June 3, 2011.

Correspondence:
Loïc Dupré, INSERM U1043, Purpan University Hospital, 31300 Toulouse, France.
Phone: international +33.0562744588.
Fax: international +33.0562744558.
E-mail: loic.dupre@inserm.fr

The online version of this article has a Supplementary Appendix.

ABSTRACT

Background
T-cell activation relies on the assembly of the immunological synapse, a structure tightly regulated by the actin cytoskeleton. The precise role of the Wiskott-Aldrich syndrome protein, an actin cytoskeleton regulator, in linking immunological synapse structure to downstream signaling remains to be clarified.

Design and Methods
To address this point, $CD4^+$ T cells from patients with Wiskott-Aldrich syndrome were stimulated with antigen-presenting cells. The structure and dynamics of the immunological synapse were studied by confocal and video-microscopy.

Results
Upon stimulation by antigen-presenting cells, Wiskott-Aldrich syndrome protein-deficient T cells displayed reduced cytokine production and proliferation. Although Wiskott-Aldrich syndrome T cells formed conjugates with antigen-presenting cells at normal frequency and exhibited normal T-cell receptor down-regulation, they emitted actin-rich protrusions away from the immunological synapse area and their microtubule organizing center failed to polarize fully towards the center of the immunological synapse. In parallel, abnormally dispersed phosphotyrosine staining revealed unfocused synaptic signaling in Wiskott-Aldrich syndrome T cells. Time-lapse microscopy confirmed the anomalous morphology of Wiskott-Aldrich syndrome T-cell immunological synapses and showed erratic calcium mobilization at the single-cell level.

Conclusions
Taken together, our data show that the Wiskott-Aldrich syndrome protein is required for the assembly of focused immunological synapse structures allowing optimal signal integration and sustained calcium signaling.

Key words: T lymphocytes, Wiskott-Aldrich syndrome, immunological synapse.

Citation: Calvez R, Lafouresse F, De Meester J, Galy A, Valitutti S, and Dupré L. The Wiskott-Aldrich syndrome protein permits assembly of a focused immunological synapse enabling sustained T-cell receptor signaling. Haematologica 2011;96(10):1415-1423. doi:10.3324/haematol.2011.040204

Introduction

Adaptive immunity relies on specific antigen recognition by T cells. Rapidly moving T cells scan secondary lymphoid organs in search for antigen-presenting cells (APC). Upon cognate antigen encounters through their T-cell receptors (TCR), T cells stop and spread on the APC to form a prolonged contact known as the immunological synapse (IS).[1,2] The molecular organization at the IS regulates TCR signal integration and subsequent T-cell activation.[3] Importantly, integrity of the actin cytoskeleton is necessary for IS assembly and sustained signal integration.[4,5] However, it remains poorly understood how the actin cytoskeleton regulates IS architecture and stability precisely, as well as early signaling events.

Multiple actin-regulatory proteins control specific actin remodeling patterns and dynamics at the IS.[6] Among them, the hematopoietic-specific actin regulator Wiskott-Aldrich syndrome protein (WASP) is of particular interest because its deficiency results in severe immunodeficiency as a consequence of multiple cellular defects.[7] WASP is known to regulate T-cell activation, as revealed by reduced proliferation and cytokine production in T cells from Wiskott-Aldrich syndrome (WAS) patients following TCR triggering.[8] The protein is normally rapidly recruited to the plasma membrane in association with lipid rafts[9] and is activated by GTP-bound Cdc42 at the site of TCR stimulation.[10] WASP nucleates actin through the Arp2/3 complex, which forms new actin branches on the sides of existing actin filaments. The assembly of a branched actin network allows the formation of lamellipodial membrane extensions that build the leading edge of migrating T cells and the peripheral ring of T cells that spread on the APC surface during IS formation.[3,11,12] The WASP-family protein WAVE2, rather than WASP itself, appears essential for the assembly of the T-cell lamellipodium and the IS, thereby putting in question the precise function of WASP during T-cell morphology remodeling in the context of antigen recognition.[13] The role of WASP at the IS has been studied using naïve T cells from different TCR transgenic WASP-KO mice. Conflicting results have been obtained concerning whether WASP regulates actin polymerization at the IS and whether it is required for conjugate formation and correct IS assembly.[14,15] Real-time observation of WASP-KO T cells on lipid bilayers presenting peptide-MHC complexes has recently revealed that WASP acts as a stabilizer of IS symmetry.[16] However, the role of WASP at the IS has been further challenged by the discovery that this protein can also be present in the nucleus, where it participates in the regulation of cytokine gene transcription.[17] In this context, the real-time observation of WASP-deficient T cells contacting APC is still missing and would help to elucidate whether WASP links IS dynamics and architecture to downstream T-cell signaling and activation.

In this study we employed time-lapse and 3-dimensional (3-D) microscopy approaches to study $CD4^+V\beta2^+$ T-cell lines derived from WAS patients, following stimulation with Epstein-Barr virus (EBV)-transformed B cells loaded with the superantigen TSST-1. This allowed us to define how WASP deficiency affects IS structure and early T-cell activation.

Design and methods

$CD4^+V\beta2^+$ T-cell lines

$CD4^+V\beta2^+$ T-cell lines were established from blood samples of two WAS patients known to have defective WASP expression (patient WAS1 was reported by De Meester *et al.*[18] and patient WAS2 by Dupre *et al.*[9]). Blood samples from healthy donors were used as controls. Blood samples from patients and healthy donors were obtained following standard ethical procedures (Helsinki protocol) and with the approval of the relevant Internal Review Boards. Details on the $CD4^+V\beta2^+$ T-cell lines and the JY cells used as APC are provided in the *Online Supplementary Design and Methods*.

Analysis of Wiskott-Aldrich syndrome protein expression by western blot

T lymphocytes were lysed for 30 min on ice in a modified RIPA buffer containing 50 mM Tris-HCl, pH 8, 150 mM NaCl, 1% IGEPAL, 1% sodium deoxycholate, 1 mM EDTA, 0.2 mM AEBSF, 1 mM Na_3VO_4, 1 mM NaF and a protease inhibitor cocktail (Sigma Aldrich). After clearing the supernatants by centrifugation, lysates were boiled in reducing sample buffer, separated through 7.5% SDS-polyacrylamide and transferred onto nitrocellulose membranes. Membranes were blocked with Odyssey blocking buffer (LI-COR Biosciences, Nebraska, USA) and incubated overnight at 4°C with anti-WASP (H250, Santa Cruz) and anti-β-actin (AC15, Sigma) antibodies. After washing, goat anti-rabbit IgG-IR Dye 800CW (LI-COR Biosciences) and goat anti-mouse-Alexa Fluor680 monoclonal antibodies (Molecular Probes) were added. WASP and β-actin expression was visualized and recorded on an Odyssey Infrared Imaging System (LI-COR Biosciences).

Proliferation

T cells (2×10^6/mL) were incubated with 2.5 μM CFSE in serum-free medium for 8 min at 37°C. Labeling was then quenched with ice-cold RPMI/5% HS before washing the cells by centrifugation. CFSE-labeled T cells (1×10^5) were then mixed with JY cells (1×10^5), preloaded or not with the indicated concentration of TSST-1, in 96-well plates. Alternatively, CFSE-labeled T cells were stimulated with phytohemagglutinin (1 μg/mL) and human interleukin-2 (100 IU/mL). Proliferation was assessed after 3 days by analysis of the CFSE dilution on a BD FACScalibur and data were analyzed using FlowJo software.

Confocal microscopy analysis of immunological synapse assembly

$CD4^+$ T cells (1×10^5) were mixed with JY cells (1×10^5) which were either unpulsed or pulsed with 10 ng/mL TSST-1, centrifuged for 2 min at 1500 rpm and incubated for 10 min at 37°C to allow conjugate formation. Cell conjugates were then allowed to sediment onto poly-L-lysine coated slides (Erie Scientific). After a total incubation time of 10, 25 or 60 min, cells were fixed for 15 min at room temperature with 3% paraformaldehyde and subsequently permeabilized with 0.1% saponin, 3% bovine serum albumin. One part of the cell conjugates was stained with phalloidin-AlexaFluor-488 (Molecular Probes) and with anti-WASP antibodies (H-250; Santa Cruz Biotechnology, Inc.) followed by donkey anti-rabbit-AlexaFluor-555 antibodies (Invitrogen). Another part of the cell conjugates was stained with anti-α-tubulin IgG1 monoclonal antibodies (Sigma) followed by goat anti-mouse IgG1-AlexaFluor-488 antibodies (Invitrogen), anti-phosphotyrosine IgG2b monoclonal antibodies (clone pY99 from Santa Cruz Biotechnology) followed by goat anti-mouse IgG2b-AlexaFluor-633 antibodies (Invitrogen) and anti-CD45 IgG2a monoclonal antibodies (clone 9.4 produced from an hybridoma from the ATCC, Manassas, VA, USA) followed by goat anti-mouse IgG2a-AlexaFluor-546 antibodies. Slides were mounted with Vectashield mounting medium (Vector Laboratories). Randomly selected conjugates were examined with a LSM 710 confocal microscope equipped with a x63-1.4 oil immersion Plan-Apochromat objective (Carl Zeiss AG, Jena, Germany).

Analysis of calcium mobilization

B-EBV cells (JY) were loaded with 10 ng/mL TSST-1 for 1 h at 37°C and then stained with 2 μM DDAO. Washed DDAO-labeled JY cells were then seeded onto poly-L-lysine-coated LabTek glass slides and incubated for 1 h at 37°C. In the mean time, T cells were labeled with 1 μM Fluo-4-AM (Molecular Probes) for 45 min at 37°C, washed and then dropped onto the JY-coated slides. Fluorescence measurements were done at 37°C/5% CO_2, on a Zeiss LSM-510 confocal microscope equipped with a x63-1.4 oil immersion Plan-Apochromat objective (Carl Zeiss AG). Images were collected with a zoom of 0.7, recorded every 17.9 sec and processed using the LSM software. The stability of T-cell/APC contacts was assessed by counting the proportion of T cells staying for 25 min within one cell diameter of their initial position, relative to the APC. To quantify changes in intracellular calcium concentration ($[Ca^{2+}]_i$) at the single cell level, T cells were incubated with 2.5 μM Fura 2-AM (Molecular Probes) for 45 min at 37°C in Hepes-buffered RPMI supplemented with 5% fetal calf serum. TSST-1-pulsed JY cells (10 ng/mL) were allowed to adhere to poly-L-lysine-coated LabTek glass slides for 1 h at 37°C, before the addition of the Fura-2-loaded T cells. Fluorescence measurements were done at 37°C/5% CO_2 on a Zeiss axiovert 200M inverted microscope equipped with a charge-coupled device camera (Princeton Instruments, Trenton, NJ, USA), an arc-xenon lamp, a computer-controlled monochromator (TILL Photonics, Planegg, Germany) and a 40× oil-objective at 37°C, 5% CO_2. Cells were sequentially excited at 340 and 380 nm every 5 sec by the monochromator. The 510 nm-emission was collected with the charge-coupled device camera and analyzed with the calcium-imaging software, Metafluor (Universal Imaging, West Chester, PA, USA). Calculation of the 340 nm to 380 nm ratios corresponding to $[Ca^{2+}]_i$ rises was done on T cells forming prolonged conjugates with APC.

Results

Human CD4+ T cells require Wiskott-Aldrich syndrome protein for optimal activation by superantigen-loaded antigen-presenting cells

Untransformed $CD4^+V\beta2^+$ T cells from a healthy donor and a WASP-deficient WAS patient (Figure 1A-B) were compared for their ability to proliferate and produce cytokines in response to EBV-transformed B cells loaded with different concentrations of TSST-1, a superantigen known to stimulate $CD4^+V\beta2^+$ T cells. In contrast to control $CD4^+$ T cells, WASP-deficient $CD4^+$ T cells failed to proliferate in response to a dose of 1 ng/mL TSST-1 (Figure 1C). Although they did proliferate at higher doses (10 and 100 ng/mL), both the proportion and the number of cell divisions were reduced when compared to control cells (Figure 1C and *Online Supplementary Figure S1A*). The intrinsic ability of WAS T cells to proliferate was not affected since they proliferated normally in response to phytohemagglutinin plus interleukin-2 (Figure 1C). It is noteworthy that the proliferative capacity of WAS $V\beta2^+$ $CD4^+$ T cells upon APC stimulation was found to be less severely affected than that observed following stimulation with immobilized anti-CD3/CD28 monoclonal antibodies (*Online Supplementary Figure S1A-B*). The reduced proliferative capacity of WAS $V\beta2^+$ $CD4^+$ T cells was directly attributable to the lack of WASP expression since re-expression of WASP by means of a lentiviral vector led to improved APC- and anti-CD3/CD28 monoclonal antibody-evoked proliferation (*Online Supplementary Figure S2A-B*). In line with the proliferative defect, when compared to T cells from healthy donors, only half of the WAS T cells produced interleukin-2 at all the TSST-1 doses tested (*Online Supplementary Figure S3*). The proportion of WAS cells that produced interferon-γ following TSST-1 stimulation was only moderately affected. More importantly, the amount of cytokines (interleukin-2 and interferon-γ) produced per cell, as assessed by mean fluorescence intensity, was strongly reduced in the WAS T cells at each dose of TSST-1 (*Online Supplementary Figure S3*). The intrinsic ability of the WAS T cells to produce interleukin-2 and interferon-γ did not, however, appear to be compromised, since PMA/ionomycin stimulation resulted in similar percentages of healthy donors' cells and WAS T cells producing cytokines. These data extend previous findings in the murine model of WAS[15] by showing that, in the context of APC stimulation, human $CD4^+$ T cells require WASP for optimal activation.

Aberrant morphology of Wiskott-Aldrich syndrome protein-deficient T cells upon contact with antigen-presenting cells

Given the actin reorganization activity of WASP, we studied the morphology of WAS $CD4^+$ T cells at contact with APC, following staining of fixed conjugates with fluorescent phalloidin. A majority of control T cells entering in contact with unpulsed APC had a round morphology and F-actin was distributed as cortical actin and within short filopodia (morphological category "inert", Figure 2A-B). In contrast, a majority of WAS T cells contacting unpulsed APC displayed activated morphological appearances, including either distorted shapes with actin protrusions away from the APC (morphological category "distorted") or elongated shapes wrapping the APC with one pole enriched in actin (morphological category "kinapse") (Figure 2A-B). As expected, upon contact with TSST-1-loaded APC, most control T cells displayed a round or slightly flattened shape with short actin-rich protrusions contacting the APC (morphological category "synapse", Figure 2A-B). In contrast again, the majority of WAS T cells contacting TSST-1-loaded APC belonged to the morphological categories "distorted" or "kinapse" (Figure 2A-B). The aberrant morphology of WAS T cells did not, however, result in a reduced ability to form conjugates with APC (*Online Supplementary Figure S4*). Together, these data suggest that in the context of WASP deficiency, actin reorganization and cell shape remodeling upon APC encounter do not proceed in a tightly controlled or focused way.

Wiskott-Aldrich syndrome protein-deficient CD4+ T cells fail to assemble focused immunological synapses

We then tested the hypothesis that aberrant actin reorganization and morphology of WAS $CD4^+$ T cells may result in the assembly of an IS with abnormal structure and altered signaling capabilities. The size of the mature IS formed after 25 min of conjugation and the distribution of markers of T-cell polarization (MTOC), molecular segregation (CD45) and TCR engagement (phosphorylated tyrosine, pTyr) were investigated by analyzing confocal planes spanning the center of conjugate contact areas and by visualizing 3-D reconstructions of z-stack series. In agreement with the propensity of WAS T cells to adopt a kinapse-type morphology, WAS $CD4^+$ T cells in contact with TSST-1-loaded APC appeared to have a slightly increased IS length as compared to control cells (Figures 3 and 4A). IS length

returned to normal following lentiviral vector-mediated correction of WASP expression. In both healthy donors' cells and WAS CD4+ T cells, contact with TSST-1-loaded APC induced polarization of the MTOC towards the contact area (Figure 3). However, measurement of the distance between the MTOC and IS center showed that WAS CD4+ T cells did not fully polarize their MTOC toward the IS center (Figure 4A). This defect was directly linked to WASP deficiency since transfer of WAS gene led to full MTOC polarization (Figure 4A). Stimulation of healthy donors' cells and WAS CD4+ T cells with TSST-1-loaded APC induced similarly high CD45 exclusion from the synaptic area (Figures 3 and 4A). We did, however, note that when in contact with unpulsed APC, WAS CD4+ T cells displayed a significant level of CD45 exclusion, which was not observed in control cells. Intense phosphorylation of tyrosine residues was induced in most of the healthy donors' cells and WAS CD4+ T cells upon conjugation with TSST-1-loaded APC (Figure 3). However, tyrosine phosphorylation in WAS T cells appeared to be more dispersed than that in control T cells and could be detected both inside and outside the confinements of the contact areas (Figure 3). When comparing the ratio of pTyr intensity at the IS and that outside the IS, WAS T cells were clearly less efficient than control T cells in enriching pTyr specifically at the IS (Figure 4A). The defect in focusing pTyr at the IS was directly attributed to WASP deficiency since WAS gene transfer corrected this defect. Analysis of the pTyr staining fluorescence intensity along the perimeter of WAS CD4+ T cells indicated that, in contrast to control cells, pTyr activation occurred at dispersed islands, both inside and outside the confinements of the IS area (one representative cell is shown in Figure 4B and three additional cells are shown in *Online Supplementary Figure S5A*). The dispersed pTyr activation of WAS T cells can also be well appreciated in 3-D animations from additional conjugates (*Online Supplementary Videos 1-6*). Following stimulation with superantigen-pulsed APC, normal T cells displayed a phosphorylated CD3ζ (pCD3ζ) signal at the IS appearing as dots coincident with the pTyr staining (*Online Supplementary Figure S5B-C*), thereby indicating a productive engagement of the TCR activation complex. In WAS T cells, although the signal for pCD3ζ appeared weaker, it was observed in association with the pTyr staining both inside and outside the confinements of the IS (*Online Supplementary Figure S5B-C*). These data suggest that the sites of TCR signaling follow an abnormally dispersed pattern in WAS T cells. However, this abnormal localization of TCR activation did not result in an abnormal rate of TCR down-regulation (*Online Supplementary Figure S6*). The above-mentioned data revealing incomplete polarization and unfocused activation of WAS T cells were obtained from the study of T cells engaged in conjugates with APC for the intermediate period of 25 min. To provide a kinetic assessment of the WAS T cell phenotype, MTOC polarization and pTyr activation were measured in parallel in WAS and healthy donors' T cells after 10, 25 and 60 min of APC contact. The inability of WAS T cells to fully polarise the MTOC was already present at 10 min and extended over 60 min (*Online Supplementary Figure S7*). Interestingly, WAS T cells appeared to have a fairly normal capacity to induce pTyr at the IS after 10 min of contact with superantigen-pulsed APC, but failed to maintain this marker of activation at later time points. Collectively, this spatio-temporal analysis of the IS architecture indicates that WAS T cells fail to properly polarize the MTOC towards the IS center and that although they initially activate pTyr in the confinement of the IS, they fail to sustain active signaling at the IS.

Abnormal behavior and erratic intracellular calcium mobilization in Wiskott-Aldrich syndrome CD4+ T cells upon encounter with superantigen-loaded antigen-presenting cells

Using time-lapse microscopy, we then evaluated the dynamic behavior of WAS CD4+ T cells at contact with APC. In parallel, the ability of these cells to be efficiently activated was assessed by single-cell $[Ca^{2+}]_i$ measurements. Upon encounter with a TSST-1-loaded APC, control CD4+ T cells rapidly stopped their locomotion to form prolonged and relatively stable conjugates with the APC (Figure 5A). A limited scanning activity was observed in the form of cycles of membrane protrusions and retractions at the edges of the T-cell/APC contact (*Online Supplementary Video 7*). In contrast, most WAS CD4+ T cells displayed an abnormal behavior, in agreement with the aberrant morphologies observed in fixed cells. WAS CD4+ T cells appeared prone to adopt an elongated morphology associated with prolonged migratory activity along the APC surface (Figure 5A and *Online Supplementary Video 8*). A quantitative analysis comparing 50 healthy donors' cells and 50 WAS T cells revealed that although WAS CD4+ T cells established prolonged contacts with APC, a reduced proportion of these cells was able to engage in stable contacts (Figure 5B). Since T cells had been pre-loaded with the Fluo-4 dye, we could investigate

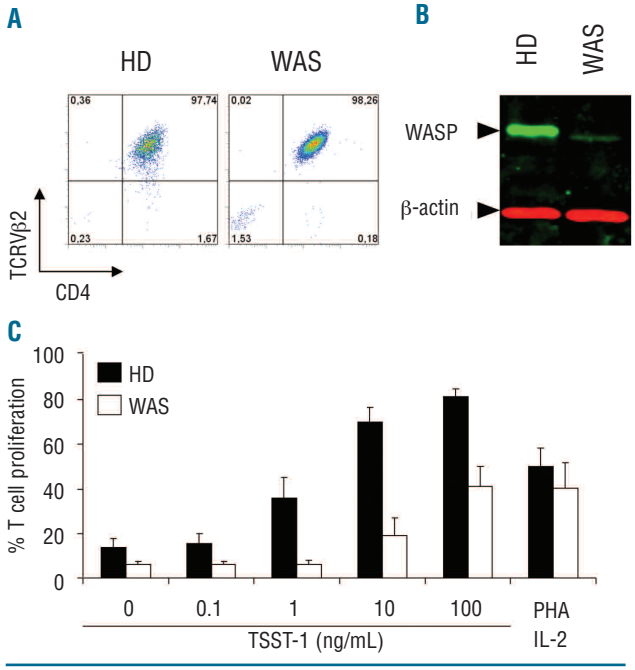

Figure 1. WASP is required for optimal APC-induced T cell activation. (A) CD4+Vβ2+ T-cell lines generated from a healthy donor (HD) and a WAS patient (WAS) were assessed for their purity. (B) WASP expression levels were confirmed in these lines by western blot analysis. (C) CFSE-labeled HD and WAS T cells were stimulated with EBV-B cells (APC) loaded with the indicated concentrations of the super-antigen TSST-1 (or PHA/IL-2, 1 μg/mL/100 IU/mL). Dilution of CFSE in dividing cells was assessed by flow cytometry 3 days after stimulation.

whether the abnormal behavior of WAS T cells on contact with APC was associated with a reduced ability to mobilize intracellular calcium. Whereas control CD4+ T cells displayed a rapid and prolonged rise in calcium as they formed a stable contact with APC, WAS CD4+ T cells showed only intermittent increases in calcium, as they were scanning the APC (Figure 5A and *Online Supplementary Video 7, 8*). To assess calcium signaling in WAS CD4+ T cells more precisely, $[Ca^{2+}]_i$ fluxes were measured at the single-cell level using the Fura-2 dye. CD4+ T cells interacting with unpulsed APC exhibited either no or only very transient patterns of calcium mobilization (*data not shown*). As shown by the representative examples depicted in Figure 5C, most control T cells exhibited a rapid and steady burst of calcium mobilization upon encountering a TSST-1-loaded APC. In contrast, WAS CD4+ T cells displayed irregular and very unstable calcium mobilization patterns, with intermittent spikes occurring periodically. A quantitative analysis comparing 13 healthy donors' cells and 16 WAS T cells revealed that the maximum $[Ca^{2+}]_i$ (usually corresponding to the rapid initial calcium rise) reached comparable values in both types of cells (Figure 5D), indicating that WAS T cells were normally sensitive to TSST-1 at the surface of the APC. However, further analysis confirmed that the calcium levels in WAS T cells were less stable than in T cells from healthy donors since the time spent above a theoretical 50% threshold (half way between maximum Fura-2 ratio and the minimum ratio) was lower in WAS T cells than in healthy donors' cells over a fixed period of time after the initial peak (Figure 5D). Furthermore, measurement of the time before a cell reached the 50% threshold after the initial burst of calcium clearly showed that WAS T cells were not able to maintain a sustained intracellular calcium level following APC contact (Figure 5F). In conclusion, our data clearly indicate that WAS

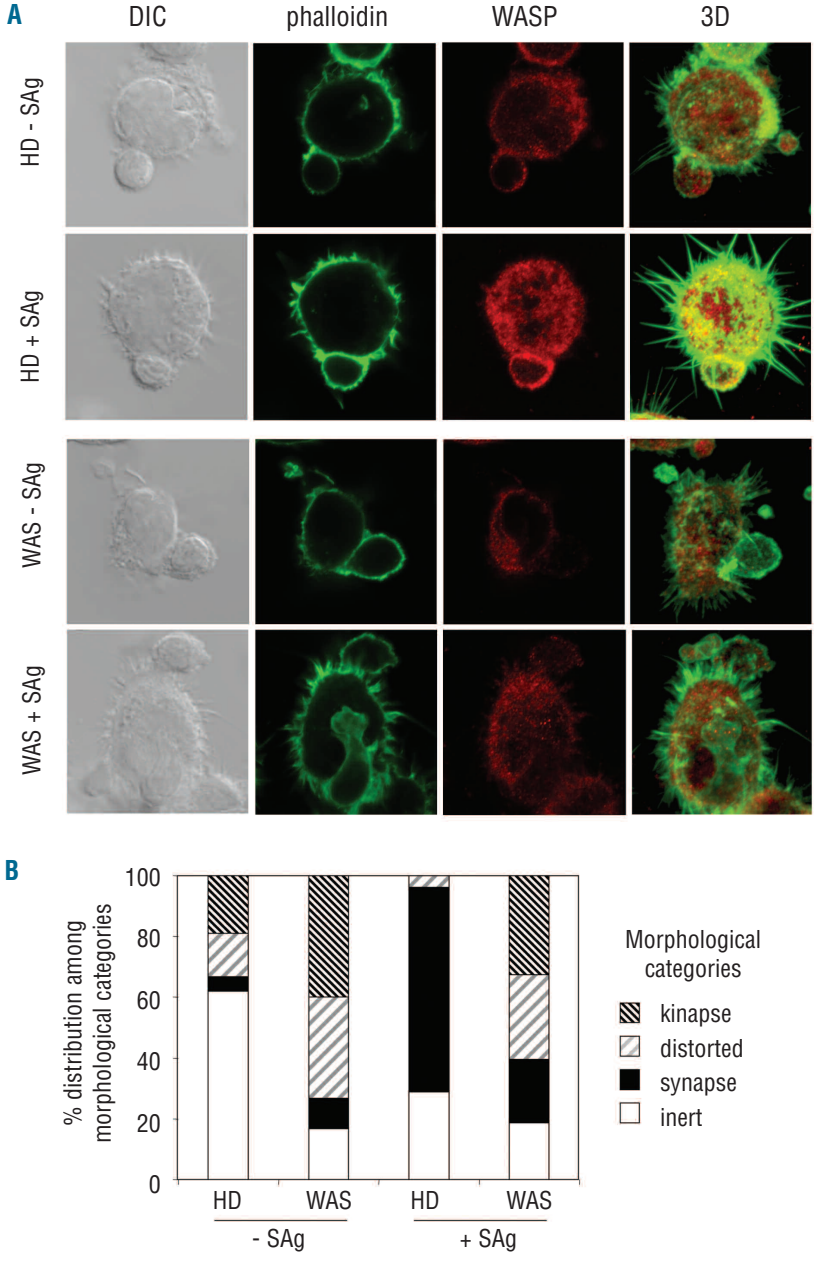

Figure 2. Abnormal morphology of WASP-deficient T cells. (A) Healthy donor (HD) and WAS CD4+Vβ2+ T cells were incubated for 30 min with APC pulsed with 10 ng/mL TSST-1 (+SAg) or not (-SAg). Cells were then fixed and stained for F-actin (green) and WASP (red). One representative T-cell/APC conjugate per condition is shown as a 3-D reconstruction from confocal sections. (B) HD and WAS T cells were classified into four morphological categories: round shape without actin-rich protrusions (inert); round or slightly flattened shape with actin-rich protrusions in contact with the APC (synapse); round to distorted shape with diverse actin protrusions away from the APC (distorted); elongated shape wrapping the APC with one pole enriched in actin (kinapse). Seventy-three T cells of each type were considered for the morphology evaluation. The presented data are representative of three experiments with one patient and three additional experiments with another patient.

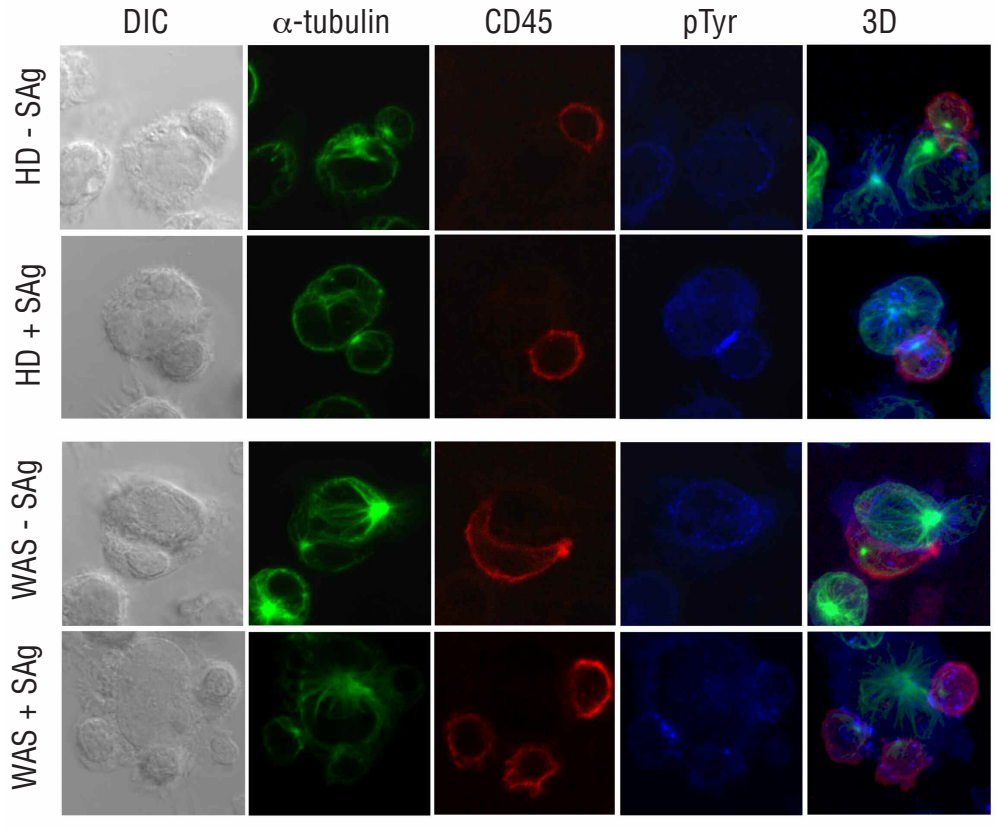

Figure 3. Structural and molecular defects at the WAS T cell IS. Healthy donor (HD) and WAS $CD4^+V\beta2^+$ T cells were incubated for 30 min with APC pulsed with 10 ng/mL TSST-1 (+SAg) or not (-SAg). Cells were then fixed and stained for α-tubulin (green), CD45 (red) and phosphotyrosine (blue). Representative T-cell/APC conjugates are shown as transmission light (DIC), confocal sections through the IS plane and 3-D reconstruction (overlay of α-tubulin, CD45 and phosphotyrosine). The presented data are from one experiment representative of six experiments. Similar data were obtained with T-cell lines from a distinct WAS patient and healthy donor.

T cells can undergo an initial rise in $[Ca^{2+}]_i$ similarly to control cells, but that they fail to maintain a sustained calcium flux, necessary for optimal T-cell activation.

Discussion

By providing a comprehensive view on the contribution of the actin regulator WASP to IS assembly, this study contributes to a better understanding of the complex interplay between actin dynamics and the regulation of TCR-driven signaling. Time-lapse and 3-D microscopy analysis of primary T-cell lines derived from WAS patients showed that WASP is required for the morphological stabilization of T cells upon APC encounter. In association with their aberrant morphology, WASP-deficient T cells assemble a poorly focused IS, characterized by incomplete polarization, spatially dispersed TCR signaling and erratic calcium mobilization. These defects may underline, at least in part, the functional defect of WAS T cells which are characterized by reduced proliferation and cytokine production.

The elongated morphology of WAS T cells upon APC conjugation supports the notion that WASP is not necessary for the formation of the lamellipodium during IS assembly, a step that appears to be under the control of the WASP-family protein WAVE2.[13] Murine models have yielded contradictory results on whether WASP participates in the cytoskeletal architecture of the IS.[14,15,19] Our live and 3-D microscopy data on T cells from WAS patients strongly support a major role of WASP in shaping the T-cell cytoskeletal architecture during an APC encounter and IS assembly. Indeed, WAS T cells display an aberrant morphology, form abnormal actin-rich protrusions and polarize their MTOC incompletely. This phenotype is consistent with the disorganized cytoskeleton polarization of WASP-deficient T cells in response to immobilized anti-CD3 monclonal antibody[20] and chemokines.[21] It is also in line with the finding that Arp2/3 knocked-down T cells produce disorganized actin-rich protrusions over the APC surface.[22] The incomplete polarization of the MTOC is also in agreement with the reduced ability of cytotoxic T lymphocytes from WAS patients to fully polarize their lytic granules towards the IS center.[18] The observation that a substantial proportion of WAS T cells is abnormally elongated and motile at the contact with APC is reminiscent of the recently described motile synapse, termed kinapse and characterized as a moving adhesive junction, with a leading lamellipodium.[23] A role for WASP in setting a synapse behavior, rather than a kinapse behavior, is supported by the finding that WASP promotes IS symmetry to counteract PKC-θ-mediated IS destabilization, in a model of naïve WASP-KO T cells interacting with lipid bilayers presenting peptide-MHC complexes.[16] However, the aberrant actin structures observed in a number of WAS T cells suggest that WASP deficiency does not simply result in the formation of physiological kinapses as an alternative to classical synapses, but rather results in the formation of non-physiological unstable synapses.

Our data show that even if WAS T cells assemble unstable synapses, they maintain the ability to form prolonged conjugates with APC, as previously reported,[13,15,24] and to engage their TCR. Activation defects in WAS T cells are, therefore, most likely related to the abnormal IS structure and molecular organization. Our study strongly suggests that WASP links controlled remodeling of actin-rich structures at the IS and positioning of the MTOC to the distribu-

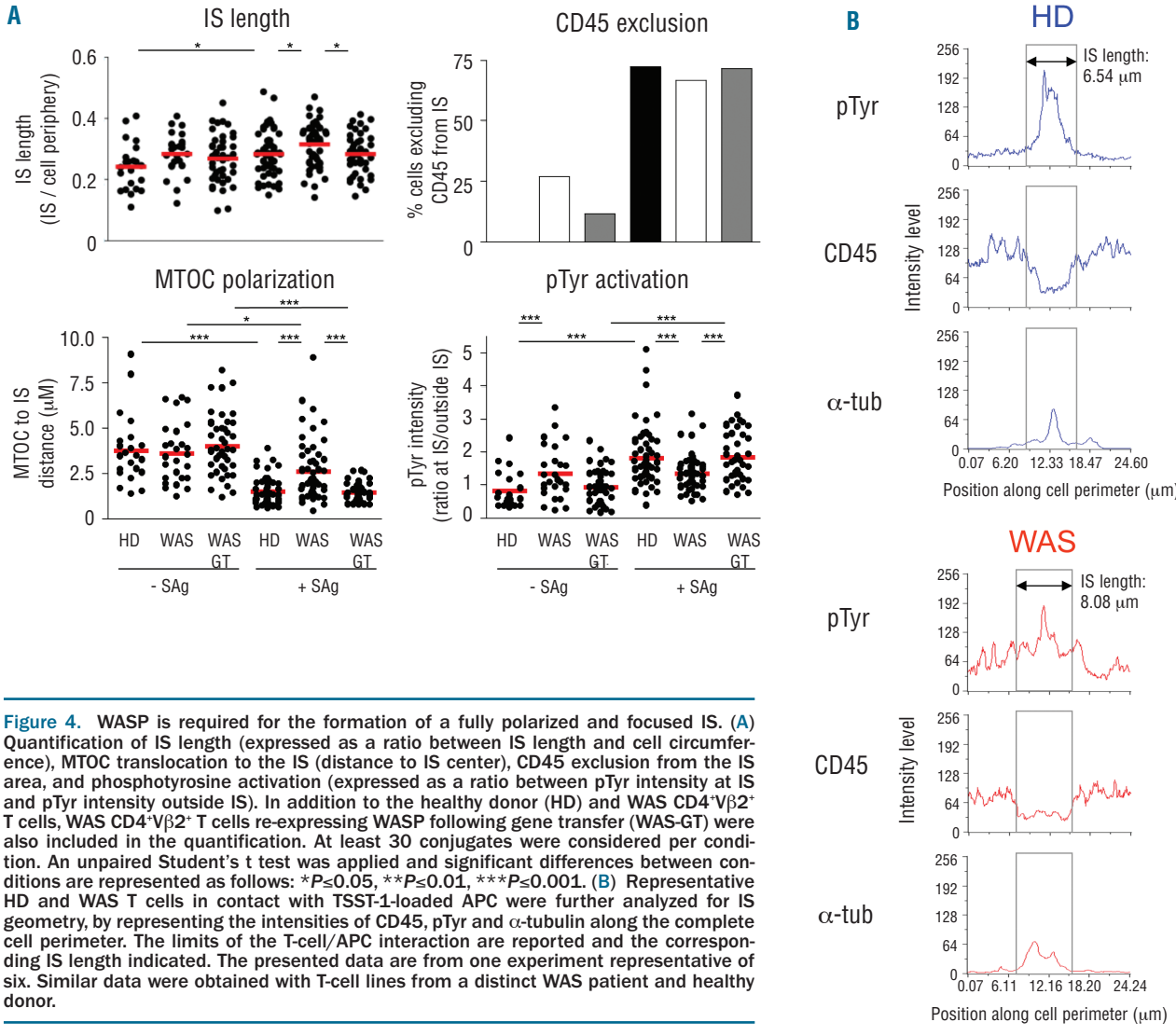

Figure 4. **WASP is required for the formation of a fully polarized and focused IS. (A) Quantification of IS length (expressed as a ratio between IS length and cell circumference), MTOC translocation to the IS (distance to IS center), CD45 exclusion from the IS area, and phosphotyrosine activation (expressed as a ratio between pTyr intensity at IS and pTyr intensity outside IS). In addition to the healthy donor (HD) and WAS CD4$^+$Vβ2$^+$ T cells, WAS CD4$^+$Vβ2$^+$ T cells re-expressing WASP following gene transfer (WAS-GT) were also included in the quantification. At least 30 conjugates were considered per condition. An unpaired Student's t test was applied and significant differences between conditions are represented as follows: *P≤0.05, **P≤0.01, ***P≤0.001. (B) Representative HD and WAS T cells in contact with TSST-1-loaded APC were further analyzed for IS geometry, by representing the intensities of CD45, pTyr and α-tubulin along the complete cell perimeter. The limits of the T-cell/APC interaction are reported and the corresponding IS length indicated. The presented data are from one experiment representative of six. Similar data were obtained with T-cell lines from a distinct WAS patient and healthy donor.**

tion of signaling complexes during TCR activation. This is in part supported by the fact that the WAS T-cell polarization defect appears to precede the activation defect. Indeed, our kinetic study indicates that the reduced ability to polarize the MTOC towards the APC is already present early after conjugate formation, while pTyr activation is normally focused within the early IS, but then becomes abnormally spread at later times. The distribution of pTyr staining outside the IS confinement in WAS T cells is in accordance with the role of Arp2/3-dependent actin remodeling in promoting central TCR/MHC accumulation.[25] Very interestingly, the actin cytoskeleton has recently been proposed to play a key role in the formation and motility of TCR microclusters observed in T cells contacting planar membrane bilayers as surrogate APC.[26] Although we could not assess whether WASP participates in actin-driven TCR microcluster dynamics in T-cell/APC conjugates, we did verify that the dots of pTyr activation were coincident with the activation of the TCR/CD3 complex, as revealed by specific staining for pCD3ζ. It remains to be investigated whether the abnormal spatial activation of WAS T cells applies to other key signaling molecules of the TCR activation complex. The dispersed distribution of TCR-driven activation may prevent coordinated signal integration, thereby resulting in the erratic pattern of calcium mobilization observed in WAS T cells. Indeed, the flux of $[Ca^{2+}]_i$ has been shown to result from the collection of individual TCR stimulation events occurring at the IS.[27] If, in addition, one considers the high motility of WAS T cells on APC, it is possible that the dispersed foci of pTyr are transient and only deliver short shots of activation. Such a dispersed and transient activation pattern could prove sufficient to induce efficient TCR internalization, similarly to the situation described for motile naïve T cells in lymph nodes.[28] However, it may not enable sustained calcium mobilization. This hypothesis is supported by the finding that recently activated T cells forming kinapses *in vivo* engage their TCR efficiently but fail to accumulate the signaling molecule LAT at the IS and emit only short calcium spikes.[29] Since an initial wave of $[Ca^{2+}]_i$ is required for the stop signal[30] and since the $[Ca^{2+}]_i$ signaling pattern regulates the shape and stability of T cells contacting APC,[31] it may be argued that a primary defect in calcium mobilization is responsible for the phenotype of WAS T cells. However,

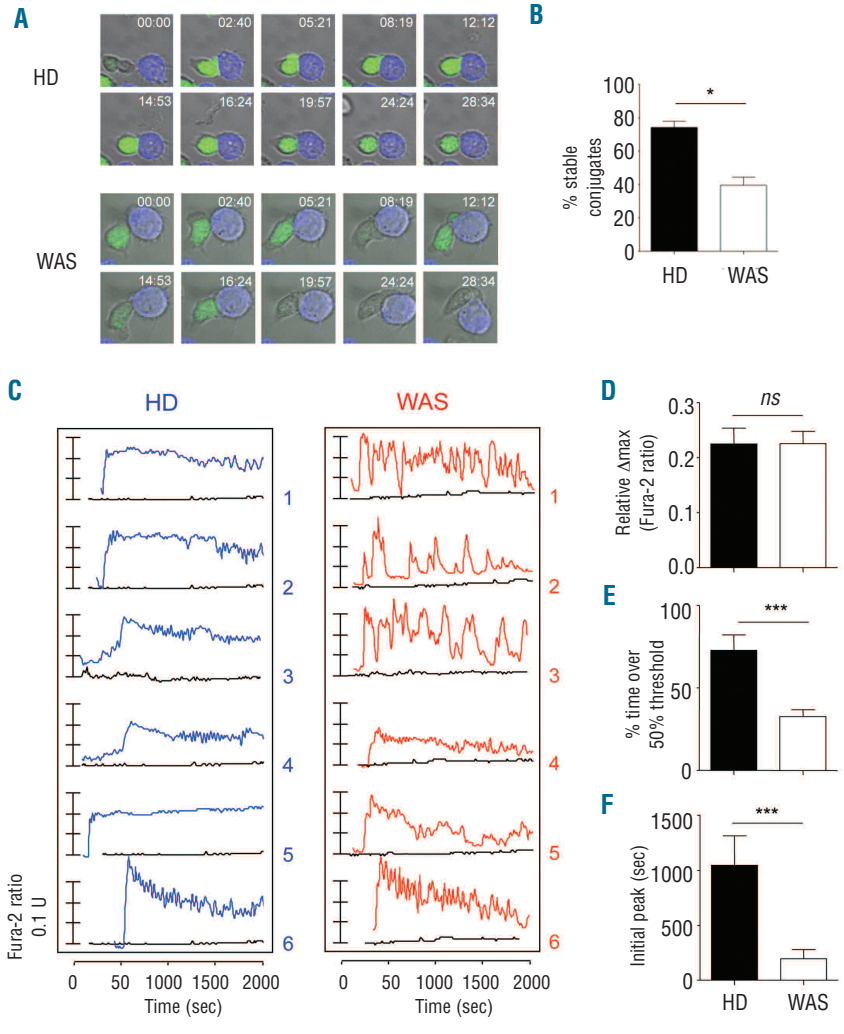

Figure 5. Erratic calcium mobilization in WAS T cells. (A) Movie sequences over 28 min 34 sec of $CD4^+V\beta2^+$ T cells from a healthy donor (HD) and a WAS patient interacting with B-EBV B cells (blue) pulsed with 10 ng/mL TSST-1. T cells were loaded with Fluo-4 to visualize the rise in intracellular calcium concentration (green). The representative HD T cell forms a relatively stable contact with the APC and displays a sustained rise in intracellular calcium, whereas the representative WAS T cell forms an unstable contact with the APC and displays intermittent rises in intracellular calcium. (B) The relative proportion of stable T/APC contacts was assessed by considering 50 HD and 50 WAS T cells contacting an APC for at least 25 min. A stable contact was defined as a T cell staying for 25 min within one cell diameter of its initial position, relative to the APC. The data shown were obtained from 18 video sequences and correspond to the mean ± SEM of three independent experiments. *P* values were calculated using a two-tailed Mann-Whitney test. (C) Measurements of the 340 nm to 380 nm ratios corresponding to $[Ca^{2+}]_i$ mobilization in six representative Fura 2-AM-labeled HD and WAS T cells forming prolonged conjugates with TSST-1-pulsed APC. (D) The relative maximum calcium variation (Δmax) per cell was calculated by subtracting the median value of the ten lowest 340/380 (Imin) ratio values to the median of the ten highest ratio values (Imax) observed in individual cells over a fixed period of time of 30 min. (E) The 50% threshold value was calculated for each individual cell over a fixed period of time (30 min) as (Imax-Imin)/2. The percent of time spent over that threshold value was then determined on a single cell basis over the same fixed period of time. (F) The initial peak duration corresponds to the amount of time the intracellular calcium ratio stayed over the 50% threshold after the initial calcium peak. Values represented in the analysis (D-F) correspond to 13 (HD) and 16 (WAS) individual T cells analyzed in a total of three independent experiments. *P* value were calculated using a two-tailed Mann and Whitney test.

the fact that WAS T cells show no defect in the intensity of the initial wave of $[Ca^{2+}]_i$, but fail to maintain sustained $[Ca^{2+}]_i$ strongly indicates that the abnormal calcium mobilization pattern is a consequence rather than a cause of the disorganized WAS T-cell IS. Previous studies have failed to detect major TCR proximal signaling defects in WASP-deficient T cells, apart from a partially reduced calcium mobilization.[9,32] Our data strongly suggest that this global reduction is due to erratic calcium mobilization at the single cell level. It is conceivable that this abnormal pattern of calcium mobilization plays a major role in the reduced activation of WASP-deficient T cells following antigen stimulation. In the context of APC, the proliferation and cytokine production defects of WASP-deficient $CD4^+$ T-cell lines appeared less pronounced than those previously observed after stimulation with anti-CD3/CD28 monoclonal antibodies (*Online Supplementary Figure 1A-B*), and would, therefore, be compatible with the observed calcium mobilization defect. In agreement, studies conducted in WASP-KO mice have shown only partially reduced to even normal T-cell proliferation or interleukin-2 production in response to APC stimulation.[15,33,34] Furthermore, reduction in proliferation and production of cytokines has been attributed to, at least in part, compromised TCR-mediated NFAT-transcriptional activation,[8,35] a pathway highly sensitive to fluctuations in $[Ca^{2+}]_i$.[36]

In conclusion, our study shows that, following an APC encounter, the actin regulator WASP controls spatial confinement of TCR activation at the IS. Our data further link focused TCR activation to sustained calcium flux and downstream activation. In apparent contrast with our findings, a role for WASP in the nucleus of T cells has been recently established, showing that it controls the transcriptional regulation of T-bet at the chromatin level.[17] We, therefore, need to consider that WASP may play parallel but non-redundant roles in distinct intracellular compartments, converging towards a fine-tuning of key signaling pathways and transcriptional programs.

Authorship and Disclosures

The information provided by the authors about contributions from persons listed as authors and in acknowledgments is available with the full text of this paper at www.haematologica.org.

Financial and other disclosures provided by the authors using the ICMJE (www.icmje.org) Uniform Format for Disclosure of Competing Interests are also available at www.haematologica.org.

References

1. Monks C, Freiberg B, Kupfer H, Sciaky N, Kupfer A. Three-dimensional segregation of supramolecular activation clusters in T cells. Nature. 1998;395(6697):82-6.
2. Grakoui A, Bromley SK, Sumen C, Davis MM, Shaw AS, Allen PM, et al. The immunological synapse: a molecular machine controlling T cell activation. Science (New York, NY). 1999;285(5425): 221-7.
3. Dustin ML. The cellular context of T cell signaling. Immunity. 2009;30(4):482-92.
4. Valitutti S, Dessing M, Aktories K, Gallati H, Lanzavecchia A. Sustained signaling leading to T cell activation results from prolonged T cell receptor occupancy. Role of T cell actin cytoskeleton. J Exp Med. 1995; 181(2):577-84.
5. Dustin ML, Cooper JA. The immunological synapse and the actin cytoskeleton: molecular hardware for T cell signaling. Nat Immunol. 2000;1(1):23-9.
6. Billadeau DD, Nolz JC, Gomez TS. Regulation of T-cell activation by the cytoskeleton. Nat Rev Immunol. 2007;7(2): 131-43.
7. Thrasher AJ, Burns SO. WASP: a key immunological multitasker. Nat Rev Immunol. 2010;10(3):182-92.
8. Trifari S, Sitia G, Aiuti A, Scaramuzza S, Marangoni F, Guidotti LG, et al. Defective Th1 cytokine gene transcription in CD4+ and CD8+ T cells from Wiskott-Aldrich syndrome patients. J Immunol. 2006;177 (10):7451-61.
9. Dupre L, Aiuti A, Trifari S, Martino S, Saracco P, Bordignon C, et al. Wiskott-Aldrich syndrome protein regulates lipid raft dynamics during immunological synapse formation. Immunity. 2002;17(2): 157-66.
10. Cannon J, Labno C, Bosco G, Seth A, McGavin H, Siminovitch K, et al. WASP recruitment to the T cell:APC contact site occurs independently of Cdc42 activation. Immunity. 2001;15(2):249-59.
11. Bunnell SC, Kapoor V, Trible RP, Zhang W, Samelson LE. Dynamic actin polymerization drives T cell receptor-induced spreading: a role for the signal transduction adaptor LAT. Immunity. 2001;14(3):315-29.
12. Barda-Saad M, Braiman A, Titerence R, Bunnell SC, Barr VA, Samelson LE. Dynamic molecular interactions linking the T cell antigen receptor to the actin cytoskeleton. Nat Immunol. 2005;6(1):80-9.
13. Nolz JC, Gomez TS, Zhu P, Li S, Medeiros RB, Shimizu Y, et al. The WAVE2 complex regulates actin cytoskeletal reorganization and CRAC-mediated calcium entry during T cell activation. Curr Biol. 2006;16(1):24-34.
14. Badour K, Zhang J, Shi F, McGavin MK, Rampersad V, Hardy LA, et al. The Wiskott-Aldrich syndrome protein acts downstream of CD2 and the CD2AP and PSTPIP1 adaptors to promote formation of the immunological synapse. Immunity. 2003;18(1):141-54.
15. Cannon JL, Burkhardt JK. Differential roles for Wiskott-Aldrich syndrome protein in immune synapse formation and IL-2 production. J Immunol. 2004;173(3):1658-62.
16. Sims TN, Soos TJ, Xenias HS, Dubin-Thaler B, Hofman JM, Waite JC, et al. Opposing effects of PKCtheta and WASp on symmetry breaking and relocation of the immunological synapse. Cell. 2007; 129(4):773-85.
17. Taylor MD, Sadhukhan S, Kottangada P, Ramgopal A, Sarkar K, D'Silva S, et al. Nuclear role of WASp in the pathogenesis of dysregulated TH1 immunity in human Wiskott-Aldrich syndrome. Sci Transl Med. 2010;2(37):37ra44.
18. De Meester J, Calvez R, Valitutti S, Dupre L. The Wiskott-Aldrich syndrome protein regulates CTL cytotoxicity and is required for efficient killing of B cell lymphoma targets. J Leukoc Biol. 2010;88(5):1031-40.
19. Badour K, Zhang J, Shi F, Leng Y, Collins M, Siminovitch KA. Fyn and PTP-PEST-mediated regulation of Wiskott-Aldrich syndrome protein (WASp) tyrosine phosphorylation is required for coupling T cell antigen receptor engagement to WASp effector function and T cell activation. J Exp Med. 2004;199(1):99-112.
20. Gallego MD, Santamaria M, Pena J, Molina IJ. Defective actin reorganization and polymerization of Wiskott-Aldrich T cells in response to CD3-mediated stimulation. Blood. 1997;90(8):3089-97.
21. Gallego MD, de la Fuente MA, Anton IM, Snapper S, Fuhlbrigge R, Geha RS. WIP and WASP play complementary roles in T cell homing and chemotaxis to SDF-1a. Int Immunol. 2006;18(2):221-32.
22. Gomez TS, Kumar K, Medeiros RB, Shimizu Y, Leibson PJ, Billadeau DD. Formins regulate the actin-related protein 2/3 complex-independent polarization of the centrosome to the immunological synapse. Immunity. 2007;26(2):177-90.
23. Dustin ML. Cell adhesion molecules and actin cytoskeleton at immune synapses and kinapses. Curr Opin Cell Biol. 2007;19(5): 529-33.
24. Krawczyk C, Oliveira-dos-Santos A, Sasaki T, Griffiths E, Ohashi PS, Snapper S, et al. Vav1 controls integrin clustering and MHC/peptide-specific cell adhesion to antigen-presenting cells. Immunity. 2002; 16(3):331-43.
25. Tskvitaria-Fuller I, Rozelle AL, Yin HL, Wulfing C. Regulation of sustained actin dynamics by the TCR and costimulation as a mechanism of receptor localization. J Immunol. 2003;171(5):2287-95.
26. Campi G, Varma R, Dustin ML. Actin and agonist MHC-peptide complex-dependent T cell receptor microclusters as scaffolds for signaling. J Exp Med. 2005;202(8):1031-6.
27. Irvine DJ, Purbhoo MA, Krogsgaard M, Davis MM. Direct observation of ligand recognition by T cells. Nature. 2002;419 (6909):845-9.
28. Friedman RS, Beemiller P, Sorensen CM, Jacobelli J, Krummel MF. Real-time analysis of T cell receptors in naive cells in vitro and in vivo reveals flexibility in synapse and signaling dynamics. J Exp Med. 2010;207 (12):2733-49.
29. Azar GA, Lemaitre F, Robey EA, Bousso P. Subcellular dynamics of T cell immunological synapses and kinapses in lymph nodes. Proc Natl Acad Sci USA. 2010;107(8):3675-80.
30. Negulescu PA, Krasieva TB, Khan A, Kerschbaum HH, Cahalan MD. Polarity of T cell shape, motility, and sensitivity to antigen. Immunity. 1996;4(5):421-30.
31. Donnadieu E, Bismuth G, Trautmann A. Antigen recognition by helper T cells elicits a sequence of distinct changes of their shape and intracellular calcium. Curr Biol. 1994;4(7):584-95.
32. Zhang J, Shehabeldin A, da Cruz LAG, Butler J, Somani A-K, McGavin M, et al. Antigen receptor-induced activation and cytoskeletal rearrangement are impaired in Wiskott-Aldrich syndrome protein-deficient lymphocytes. J Exp Med. 1999;190(9): 1329-41.
33. Marangoni F, Trifari S, Scaramuzza S, Panaroni C, Martino S, Notarangelo LD, et al. WASP regulates suppressor activity of human and murine CD4(+)CD25(+)FOXP3(+) natural regulatory T cells. J Exp Med. 2007;204(2):369-80.
34. Le Bras S, Massaad M, Koduru S, Kumar L, Oyoshi MK, Hartwig J, et al. WIP is critical for T cell responsiveness to IL-2. Proc Natl Acad Sci USA. 2009;106(18):7519-24.
35. Cianferoni A, Massaad M, Feske S, de la Fuente MA, Gallego L, Ramesh N, et al. Defective nuclear translocation of nuclear factor of activated T cells and extracellular signal-regulated kinase underlies deficient IL-2 gene expression in Wiskott-Aldrich syndrome. J Allergy Clin Immunol. 2005; 116(6):1364-71.
36. Oh-hora M, Rao A. Calcium signaling in lymphocytes. Curr Opin Immunol. 2008;20 (3):250-8.